Real-time ocular artifact suppression using recurrent neural network for electro-encephalogram based brain–computer interface

A. Erfanian **B. Mahmoudi**

Department of Biomedical Engineering, Faculty of Electrical Engineering,
Iran University of Science and Technology, Narmak, Tehran-16844, Iran

Abstract—*The paper presents an adaptive noise canceller (ANC) filter using an artificial neural network for real-time removal of electro-oculogram (EOG) interference from electro-encephalogram (EEG) signals. Conventional ANC filters are based on linear models of interference. Such linear models provide poorer prediction for biomedical signals. In this work, a recurrent neural network was employed for modelling the interference signals. The eye movement and eye blink artifacts were recorded by the placing of an electrode on the forehead above the left eye and an electrode on the left temple. The reference signal was then generated by the data collected from the forehead electrode being added to data recorded from the temple electrode. The reference signal was also contaminated by the EEG. To reduce the EEG interference, the reference signal was first low-pass filtered by a moving averaged filter and then applied to the ANC. Matlab Simulink was used for real-time data acquisition, filtering and ocular artifact suppression. Simulation results show the validity and effectiveness of the technique with different signal-to-noise ratios (SNRs) of the primary signal. On average, a significant improvement in SNR up to 27 dB was achieved with the recurrent neural network. The results from real data demonstrate that the proposed scheme removes ocular artifacts from contaminated EEG signals and is suitable for real-time and short-time EEG recordings.*

Keywords—*EEG, Adaptive noise canceller, Ocular artifact, Recurrent neural network, Brain–computer interface*

Med. Biol. Eng. Comput., 2005, **43**, 296–305

1 Introduction

ELECTRO-ENCEPHALOGRAM (EEG) signals are contaminated by noise from sources such as eye blink and eye movement. The traditional method of eye blink suppression is removal of the segment of EEG data in which eye blinks occur. Eye blinks are usually detected by means of data recorded from electrodes placed above and below the subject's left eye. An eye blink is said to have occurred if the signal amplitude exceeds a given threshold. All EEG segments in which eye blinks occur are then excluded. In addition, in some event-related potential experiments, eye blinks are superimposed on evoked-response components. In this case, a common approach is to reject all EEG epochs containing a signal amplitude larger than some selected value. These schemes are rigid and do not lend themselves to adaptation. Moreover, a great number of data are lost.

Correspondence should be addressed to Dr Abbas Erfanian; email: erfanian@iust.ac.ir

Paper received 17 June 2004 and in final form 13 December 2004

MBEC online number: 20053997

Several methods based on regression in the time domain (GRATTON *et al.*, 1983) or frequency domain (WOESTENBURG *et al.*, 1983) have been proposed for removing eye blink artifacts. However, all these methods require off-line analysis that is not suitable for real-time applications. Principle component analysis (PCA) has also been proposed as a method for removing eye artifacts from multichannel EEG (BERG and SCHERG, 1991; 1994; LINS *et al.*, 1993). However, PCA cannot completely separate eye artifacts from EEG signals, especially when they have comparable amplitude (JUNG *et al.*, 2000).

Recently, a more effective method has been introduced for removing a wide variety of artifacts from multichannel EEG signals, based on blind source separation by independent component analysis (ICA) (MAKEIG *et al.*, 1996; VIGARIO, 1997). However, the method requires visual inspection of ICA components and manual classification of the interference components. This can be time-consuming and is not desirable for real-time artifact suppression. In particular, these techniques require multichannel EEG and cannot be applied to a single-channel recording.

To overcome these problems and to shorten the experimental session, the customary practice is to invoke the use of an adaptive noise canceller (ANC). The ANC, which is a special

approach to adaptive filtering, has been widely used in interference cancellation (THAKOR and YI-SHENG, 1991; LAGUNA *et al.*, 1992). HE *et al.* (2004) employed an ANC with two separate linear adaptive filters for ocular artifact cancellation. A pair of electrodes were placed above and below the eye to record the vertical electro-oculogram (EOG), and another pair of electrodes were placed at the left and right outer canthi to record the horizontal EOG. The recorded vertical EOG and horizontal EOG were used as two separate reference inputs. Each reference was first processed by an adaptive filter and then subtracted from the recorded EEG.

STROBACH *et al.* (1994) proposed an ANC for event-synchronous cancellation of ECG interference in biomedical signals using the QRS synchronously repeated estimated average waveform of the interference as an artificial reference signal. The method is applied to the cancellation of the heart interference in magneto-encephalogram (MEG) signals and to isolation of the ventricular extrasystoles in magnetocardiogram. DENG *et al.* (2000) developed an event-synchronous interference canceller for cancellation of electrocardiographic interference in diaphragmatic electromyographic signals. The trigger points created by the QRS detector are used for QRS synchronous segmentation of the corrupted MEG signals. Then, the resulting temporal segments are averaged to estimate the artificial reference signal. However, owing to the random nature of eye blinking or movement, this scheme cannot be applied to ocular artifact removal from the EEG.

All of the methods discussed above are based on linear adaptive filtering. Linear adaptive filters offer an important tool for the modelling and prediction of stochastic signals. However, linear models are generally inadequate for modelling systems with even mild non-linearities. Owing to the inherently non-linear nature of biological systems, the development of a non-linear adaptive filter (NAF) would be desirable for the adaptive processing of biomedical signals. Until now, a variety of NAFs based on Volterra series expansion (PARSA *et al.*, 1998; MATHEWS, 1991; RAUF and AHMED, 1997) and feedforward neural networks (JAMES *et al.*, 1997; GRIEVE *et al.*, 2000) have been developed and employed in various applications.

PARSA *et al.* (1998) applied both linear and non-linear adaptive noise cancellers to the problem of stimulus artifact (SA) reduction in non-cortical somatosensory evoked potentials (SEPs), where the ensemble-averaged SEP + SA composite waveform is utilised as the primary input. It was shown that the non-linear ANC, which was based on a truncated second-order Voltera series expansion, provided significantly better stimulus artifact cancellation than the linear ANC.

JAMES *et al.* (1997) used the technique of multireference adaptive noise cancelling (MRANC) to enhance non-stationarities in the EEG, with the adaptation implemented by means of a feedforward neural network. It was shown that the non-linear MRANC gave an improvement in performance compared with a linear MRANC.

GRIEVE *et al.* (2000) developed a neural network-based ANC for estimating somatosensory evoked potentials and cancelling the stimulus artifact. The primary and reference inputs used to train the network were generated by averaging of the training sets. The network was trained with a segment of recorded data that did not contain the evoked signal. The final result was obtained by averaging the results of filtering each record in the test set. However, the proposed scheme can only be employed when the stimulus artifact does not overlap the evoked potentials. Moreover, real-time artifact suppression was not considered in this work.

SADASIVAN and DUTT (1997) adopted a non-linear ANC, which was based on a second-order Volterra function, for reducing the EOG in electro-encephalography measurements. However, real-time minimisation of the ocular artifacts was not considered in this work. A non-linear ANC without a reference signal was successfully used to estimate brainstem auditory evoked potentials (ARABI and ERFANIAN, 1999). The non-linear ANC was based on a feedforward neural network. It was observed that a significant improvement in waveform estimation could be achieved by the neural network adaptive filters, compared with the ensemble-averaging and time-varying linear adaptive filter.

In our previous work (ERFANIAN and MAHMOUDI, 2002), a feedforward neural network was utilised for real-time removal of eye blink interference from EEG signals. The reference signal was collected by an electrode placed on the forehead above the eye. The reference signal was first low-pass filtered by a moving average filter and then applied to the ANC. The results showed that single-electrode recording provides satisfactory reference input correlated with the noise in the primary signal.

Our aim in this paper was to make use of the advantages of artificial neural networks in developing an adaptive noise canceller for real-time ocular artifact suppression. In this approach, we consider recurrent neural networks (RNNs). Recurrent networks have advantages over feedforward neural networks in much the same way that autoregressive moving average models have advantages over autoregressive models (CONNOR *et al.*, 1994). RNNs address the temporal relationship of their inputs by maintaining an internal state and perform dynamic mapping. Owing to this fact, we employed a recurrent neural network to predict the ocular interference and compare its performance with that of a feedforward neural network in cancelling eye blinks.

2 Methods

2.1 *Principle of ANC*

The concept of adaptive noise cancelling was proposed by WIDROW and STREANS (1985). The idea is to subtract out a filtered version of noise, known to be correlated with the noise corrupting the desired signal. The filter is continuously modified by some algorithm to optimise some performance criterion on the estimated signal. A typical structure of an adaptive noise canceller is shown in Fig. 1. The ANC has two inputs: the primary input and the reference input. The primary input x is the desired signal of interest s buried in noise v_0, as shown by

$$x(n) = s(n) + v_0(n) \tag{1}$$

The reference input contains noise v_1, which is correlated with the noise component of the primary signal but uncorrelated with the desired signal; that is,

$$E[s(n)v_1(n-k)] = 0 \quad \text{for all } k \tag{2}$$

It is assumed that the signal and noise in the primary input are uncorrelated; that is,

$$E[s(n)v_0(n)] = 0 \quad \text{for all } k \tag{3}$$

The ANC is based on adaptive filtering of the reference signal to produce an estimate of the noise component of the primary signal; that is,

$$\hat{v}_0(n) = \sum_{k=0}^{M-1} \hat{w}_k(n) v_1(n-k) \tag{4}$$

where $\hat{w}_0(n), \hat{w}_1(n) \ldots, \hat{w}_{M-1}(n)$ are the adjustable tap weights of the adaptive filter, and $v_1(n), v_1(n-1), \ldots, v_1(n-M+1)$ are the tap inputs. The output of the adaptive filter is then subtracted from the primary signal to produce an estimate of the desired signal.

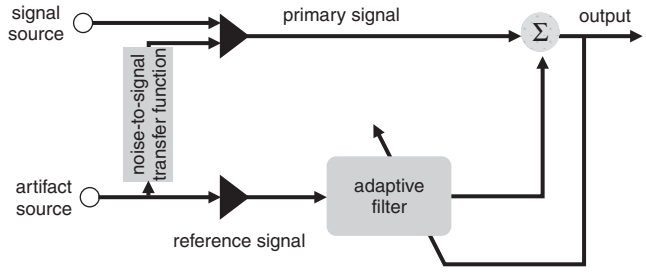

Fig. 1 *Adaptive noise canceller with reference signal*

In adaptive noise cancelling, the quality of the reference signal is the most critical factor. It should be uncorrelated with the desired signals. As the level of the crosstalk between the reference signal and desired signal increases, the performance of the ANC begins to degrade. Ensemble and moving window averages were formerly used to construct the reference input with good results (CHAN *et al.*, 1995). Recently, a Gaussian radial basis function neural network was used as a prefilter to provide a proper reference signal for adaptive filtering of evoked potentials (QUI *et al.*, 2002). In this work, we used a moving window average to preprocess the recorded reference signal to provide an effective reference input for the ANC.

2.2 *Recurrent neural network*

The recurrent neural network, which involves dynamics elements in the form of a feedback loop, has a profound impact on the learning capability of the network and on its performance (GILES *et al.*, 1994; TSOI and BACK, 1994). Moreover, the feedback loops that feed back the lagged outputs of the neurons to the inputs of the neurons enable the network to perform dynamic mapping and learning tasks that extend over time.

The architecture of the recurrent neural network takes many different forms (TSOI and BACK, 1994). In this work, we used a recurrent multilayer perceptron with a single hidden layer, as illustrated in Fig. 2. The network contained recurrent connections from the hidden neurons to a layer consisting of unit delays. The output of the unit-delay layer was fed to the input layer. We could then describe the dynamic behaviour of the network with the following equations:

$$y(t+1) = \sum_{i=1}^{q} c_i g_i(t)$$

$$g_i(t) = f\left(\sum_{j=1}^{p} w_{ji} x(t-j+1) + \sum_{k=1}^{q} v_{ki} g_k(t-1)\right) \quad (5)$$

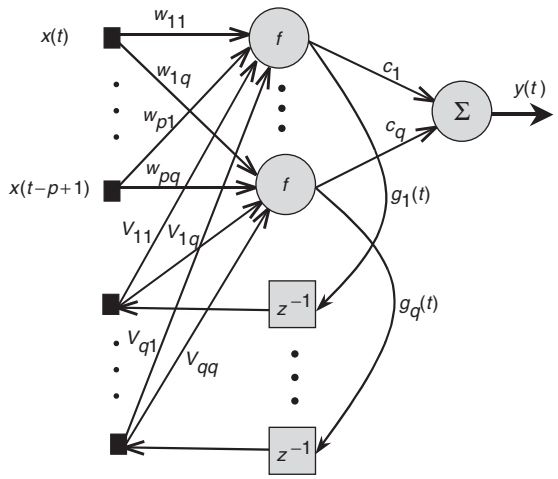

Fig. 2 *Structure of recurrent single-layer perceptron*

where $f(\cdot,\cdot)$ is a non-linear activation function characterising the hidden units, $g_i(t)$ is the response of the ith hidden unit, and c_i is its connecting weight to the output unit. The w and v are the connecting weights of the input units and unit-delay units to the hidden units, respectively. The hidden layer is non-linear, but the output layer is linear. We estimated the parameters c, w and v using the standard backpropagation learning algorithm (HAYKIN, 1999).

In this paper, we employed the RNN for adaptive noise cancelling with the reference signal for the suppression of ocular artifacts. The primary input was the recorded EEG signal contaminated by the EOG, and the reference signal was the EOG. The RNN was used for adaptive filtering of the reference signal to obtain a better model of the noise component of the primary input.

3 Simulation study

3.1 *Simulation data*

A simulation study was carried out to test the capabilities of the neural adaptive noise canceller for ocular artifact suppression. The NAF was implemented here by means of a recurrent single layer perceptron (RSLP) network with four input nodes, five hidden units with hyperbolic tangent activation function, and one linear output node.

An autoregressive process driven by Gaussian white noise simulated the ongoing EEG (YU *et al.*, 1994) as follows:

$$s(t) = 1.5084s(t-1) - 0.1587s(t-2) - 0.3109s(t-3) - 0.0510s(t-4) + w(t) \quad (6)$$

where $w(t)$ is a white-noise sequence with Gaussian distribution. The artifacts were simulated by an exponentially damped sinusoid with randomly varied amplitudes and shapes satisfying a uniform distribution. The jth artifact is thus simulated as

$$n_j(k) = Ka_j e^{-k/\tau_j} \sin(2\pi k/N) \quad \text{for } k = 0 \ldots N-1 \quad (7)$$

where N is the length of the artifact waveform and is set to 128 samples. The parameter a_j is the amplitude of the jth artifact, and τ_j is a parameter determining the shape. K is an amplitude scaling constant. To simulate the variations in amplitude and shape of the artifacts, both parameters were set to new random values at the onset of each artifact. The new values of a_j and τ_j were randomly chosen from a Gaussian distribution with ($\mu = 1$, $\sigma^2 = 0.1$) and ($\mu = 250$, $\sigma^2 = 50$), respectively. The artifacts were generated exponentially distributed over time, with the occurrence rate of 0.5 per unit time. One unit of time corresponds to 1024 samples of discrete time series. The generated artifacts were scaled and added to simulated EEG to provide the primary signal with a specific value of SNR.

The relative mean-squared error (MSE) was used to quantify the efficacy of the NAF in cancelling the ocular artifacts. The MSE is defined as

$$MSE = \frac{\sum_{k=0}^{L-1} [s(k) - \hat{s}(k)]^2}{\sum_{k=0}^{L-1} s^2(k)} \quad (8)$$

where $\hat{s}$ is the output of the NAF, and s is the signal to be estimated. The performance index is computed in each unit of time.

3.2 *Results*

The performance of the NANC in cancelling the artifacts was compared with different SNRs at the primary and the reference signals, different numbers of hidden units, and different numbers of tap inputs. In all cases, the power of the simulated artifact was adjusted to provide the desired SNR at the primary input signal. Shown in Figs. 3*a–c* are portions of simulated EEG, artifacts and the resulting primary signal, respectively. In this case, the SNR of the primary signal was set at −6 dB, and the reference signal was not contaminated by the EEG. Figs 3*d* and *e* demonstrate portions of the estimated artifact-free EEG after artifact cancellation using a standard single-layer perceptron (SSLP) with eight hidden units and a standard two-layer perceptron (SMLP) with eight units in the first hidden layer and four units in the second hidden layer, respectively. The estimated artifact-free EEG using the recurrent single layer perceptron (RSLP) with eight hidden units is shown in Fig. 3*f*. In all cases, the hidden units were nonlinear with hyperbolic activation function, but the output unit was linear.

The performance of the networks was examined with different values of the learning rate, and the optimum value was selected for each network. Fig. 4 shows the error curves of the networks for different values of the learning rate. It was found that the optimum learning rate parameter was about 0.0013 for the SSLP, 0.0005 for the SMLP and 0.0005 for the RSLP. It was seen that, as the learning rate became larger, the network learned faster initially, but the larger learning rate gave larger ripples as learning proceeded.

We also evaluated the performance of the NANCs in artifact cancelling with different orders of inputs. Fig. 5 shows the error curves of the networks for different orders. It was observed that the performance of the NANC with input $[r(t), r(t-1), r(t-2), r(t-3)]$ was better than that with input $[r(t), r(t-1)]$ or $[r(t), r(t-1), r(t-2), r(t-3), r(t-4), r(t-5)]$.

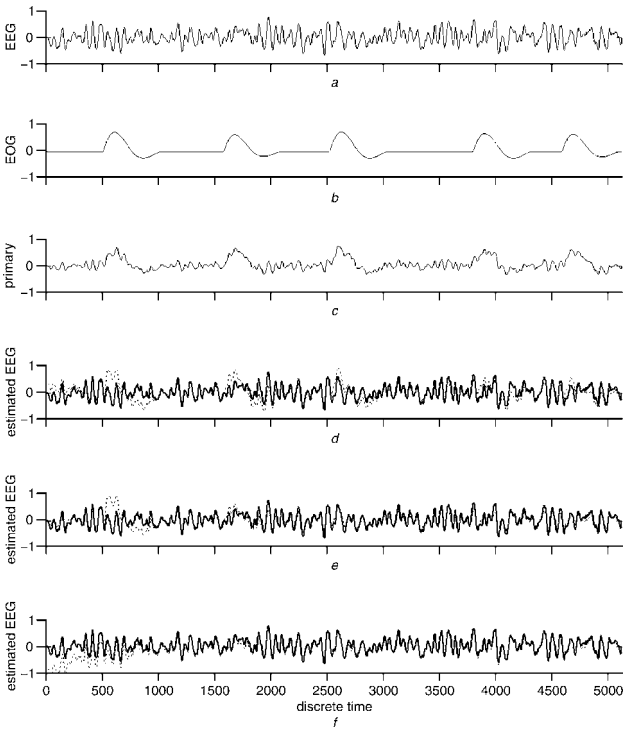

Fig. 3 *(a) Simulated EEG. (b) Simulated artifacts. (c) Simulated primary signal (SNR = −6 dB). (·····) Estimated artifact-free EEG using (d) SSLP with 8 hidden units, (e) SMLP with 8 units in first hidden layer and 4 units in second hidden layer, and (f) RSLP with 8 hidden units*

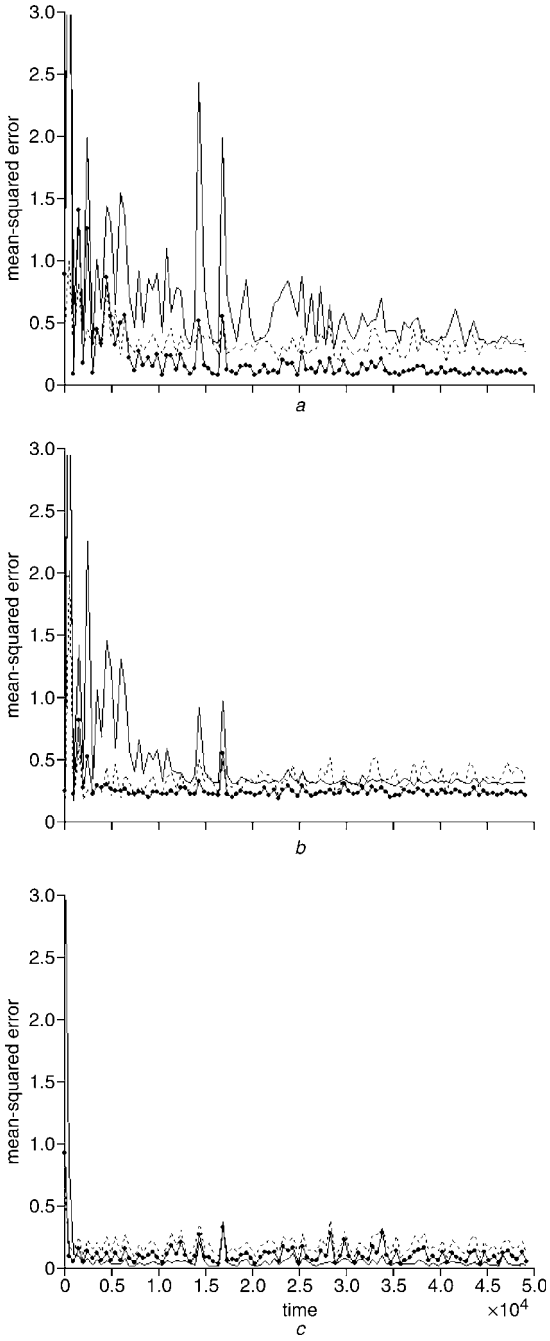

Fig. 4 *Error curves of (a) SSLP, (b) SMLP and (c) RSLP for different values of learning rate. (a) Learning rate: (——) 0.0001; (-●-●-●) 0.001; (·····) 0.01. (b) Learning rate: (——) 0.0001; (-●-●-●) 0.0005; (·····) 0.005. (c) Learning rate: (——) 0.0005; (-●-●-●) 0.001; (·····) 0.003*

Moreover, it was found that increasing the number of hidden units did not result in a significant improvement in performance.

Fig. 6 shows the same information as in Fig. 3 when the SNR of the primary signal is set at −8 dB. It was observed that, in spite of the random variations in amplitude, shape and occurrence of artifacts, and different SNRs, a perfect cancellation was achieved using the RSLP.

Fig. 7 shows the error curves for different SNRs of the primary signal during adaptive noise cancelling using RSLP, SSLP and SMLP. An overall SNR improvement of 16, 7 and 27 dB is achieved by using SSLP, SMLP and RSLP, respectively. From the above, it is found that RSLP was suitable for artifact suppression under different SNRs. Moreover, the performance of the recurrent neural network was much better than that of the feedforward network. Even with four inputs

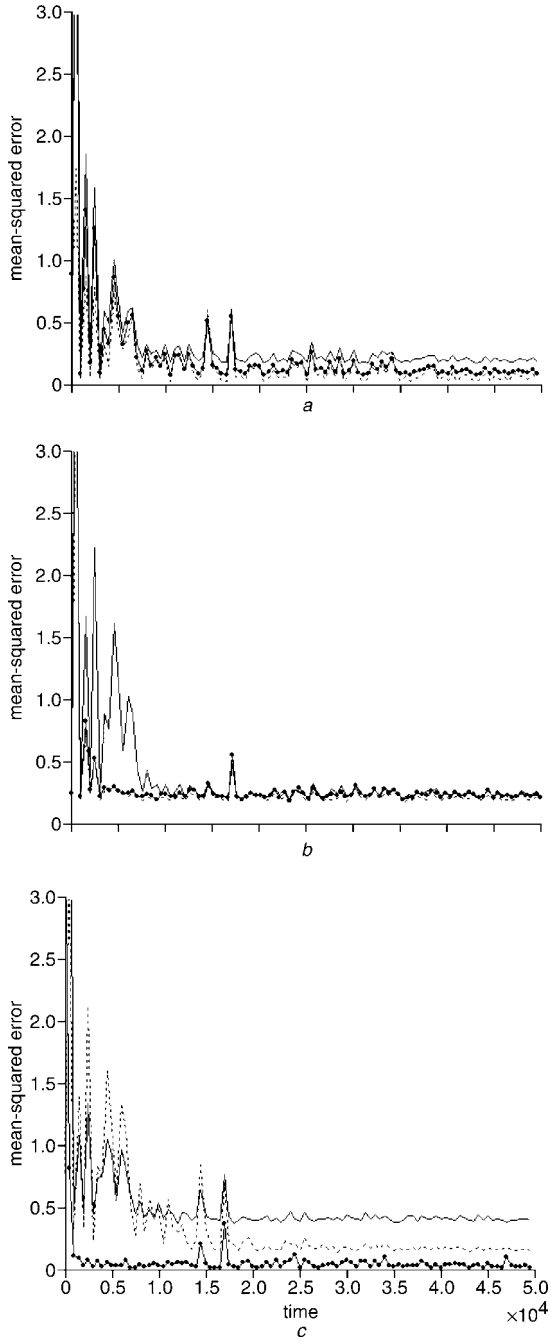

Fig. 5 *Error curves of (a) SSLP, (b) SMLP and (c) RSLP for input order (——) [r(t), r(t − 1)], (-•-•-•) [r(t), r(t − 1), r(t − 2), r(t − 3)] and (·····) [r(t), r(t − 1), r(t − 2), r(t − 3), r(t − 4), r(t − 5)]*

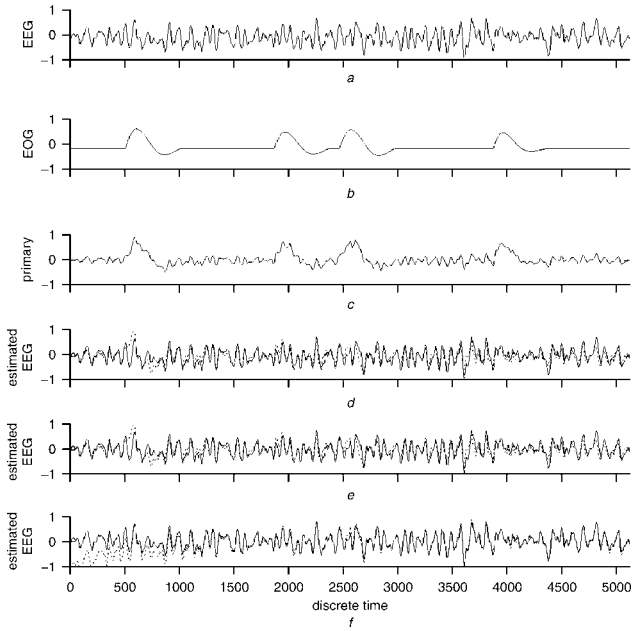

Fig. 6 *(a) Simulated EEG. (b) Simulated artifacts. (c) Simulated primary signal (SNR = −8 dB). (·····) Estimated artifact-free EEG using (d) SSLP with 8 hidden units, (e) SMLP with 8 units in first hidden layer and 4 units in second hidden layer and (f) RSLP with 8 hidden units*

and only eight hidden units (48 parameters in total), the RSLP performed better than the feedforward network with two hidden layers, eight units in the first hidden layer and four units in the second hidden layer (84 parameters in total).

3.3 *Effect of EEG interference in reference input*

As mentioned above, to establish a perfect cancelling of the interference, the quality of the reference signal is the most important factor. However, the reference signal is also contaminated by the EEG signals. Here, a moving window average of order 64 was used to reduce the EEG interference. To investigate the performance of the NANC in cancelling the artifacts during EEG interference, the simulated EEG was added to the simulated artifacts to provide the reference signals. Figs 8*a–d* show the portion of simulated EEG, artifacts and resulting primary and reference signals, when the SNR of the primary and reference signal was set at −6 dB and 10 dB, respectively. The estimated artifact-free EEG signal using RSLP with and without the moving averaged filter is shown Figs 8*e* and *f*, respectively. It was observed that prefiltering the reference signal significantly improved the performance of the NANC. It is clear that the NANC with prefiltering of the reference signal can best suppress the artifacts. The MSE of the NANC without prefilter was much larger than that of the NANC with prefilter.

3.4 *Effect of non-linear EOG-to-EEG transfer*

All the results described above were based on the assumption that the EOG-to-EEG transfer was linear. In this Section, we assume that the EOG-to-EEG transfer was non-linear. The simulated artifacts were added to simulated EEG in a non-linear way to provide the simulated primary signal as

$$x(t) = EEG(t) + \alpha\xi(EOG(t)) \tag{9}$$

where α is the scaling factor, and ξ is the non-linear transfer, which was chosen to be of the form (SADASIVAN and DUTT (1997))

$$\xi(EOG(t)) = EOG(t) + EOG^2(t) + EOG^3(t) \tag{10}$$

Figs 9*a–d* show the portion of simulated EEG, EOG, $\xi(EOG)$ and the resulting primary signal, respectively. The simulated $\xi(EOG)$ was scaled and added to the simulated EEG to produce an SNR of −6 dB. Fig. 9*e* shows the estimated artifact-free EEG using RSLP with eight hidden units. We can clearly observe that the non-linear filter would be able to identify the non-linear EOG-to-EEG channel in a short convergence time and effectively remove the artifacts.

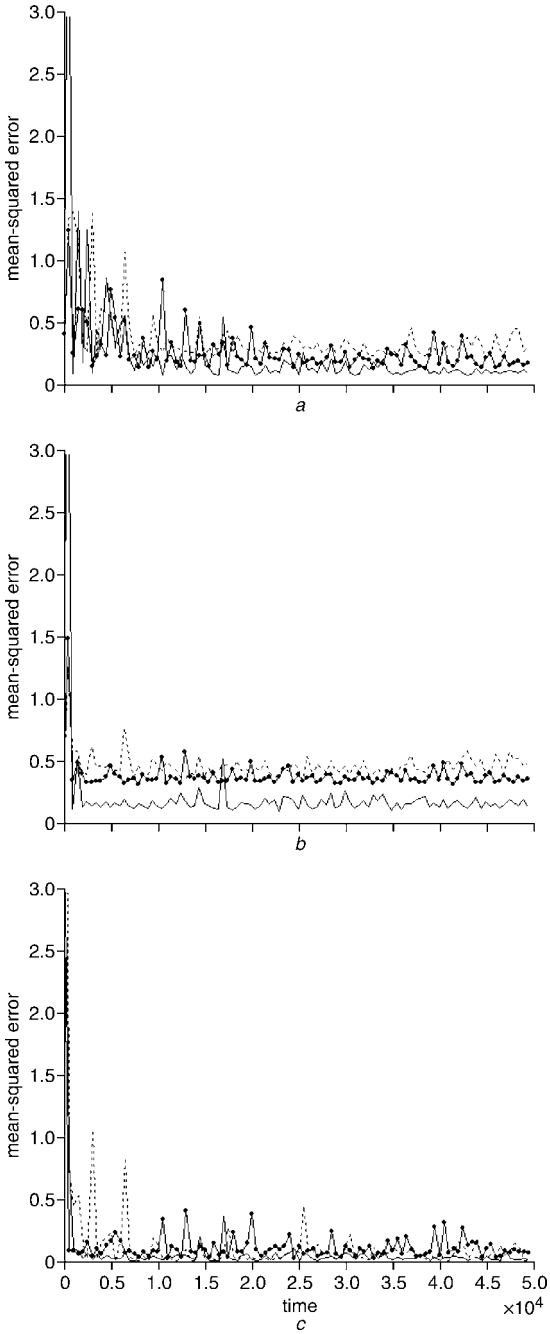

Fig. 7 *Error curves of (a) SSLP, (b) SMLP and (c) RSLP for different SNRs of primary signal. SNR: (——) − 6 dB; (-•-•-•) − 8 dB; (·····) − 10 dB*

4 Real data acquisition and real-time processing

4.1 *Hardware and software*

The overall system comprised an IBM-compatible 1.7 GHz Pentium IV personal computer, eight-channel EEG amplifier and a high-performance data acquisition card*. To implement such a real-time BCI on a PC, appropriate computer software was required. The software had to handle on-line data acquisition and real-time processing. In our case, we used Matlab Simulink (THE MATHWORKS, 1998–2000), Real-Time Workshop (THE MATHWORKS, 1999–2000), and Real-Time Windows Target under Windows 98 for on-line data acquisition, filtering and ocular artifact suppression. Simulink provides an interactive environment for modelling, simulating, controlling

*PCL-818HG, Advantech

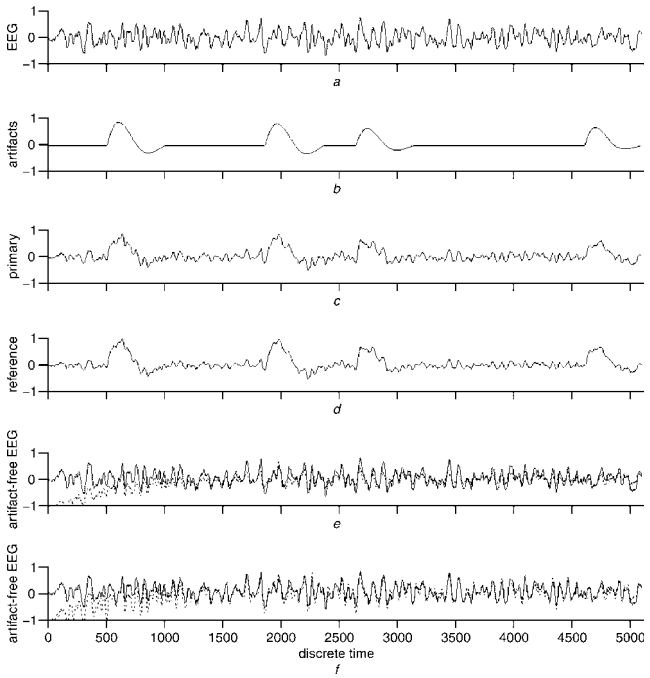

Fig. 8 *(a) Simulated EEG. (b) Simulated artifacts. (c) Simulated primary signal (SNR = −6dB). (d) Simulated reference signal (SNR = 10 dB). (·····) Estimated artifact-free EEG using RSLP with 8 hidden units, (e) with and (f) without moving averaged filter*

and processing as a block diagram using predefined blocks. Real-Time Workshop provides the tools for converting Simulink models into C code and then compiling the code into a real-time executable using a C compiler. The executable code is loaded into memory, and the Real-Time Windows target kernel runs the code in real time.

4.2 *Real-time ocular artifact suppression*

The EEG data of normal subjects were recorded at a sampling rate of 256 Hz by Ag/AgCl scalp electrodes. The

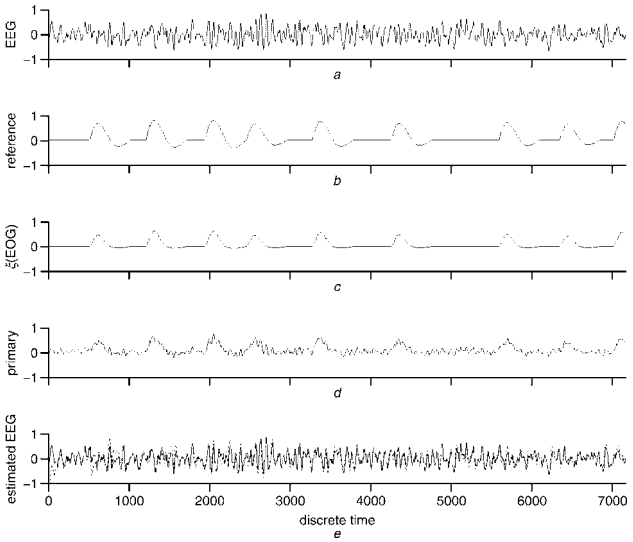

Fig. 9 *(a) Simulated EEG. (b) Simulated reference signal (EOG). (c) Simulated ξ(EOG). (d) Simulated primary signal (SNR = −6dB). (e) (·····) Estimated artifact-free EEG using RSLP with 8 hidden units*

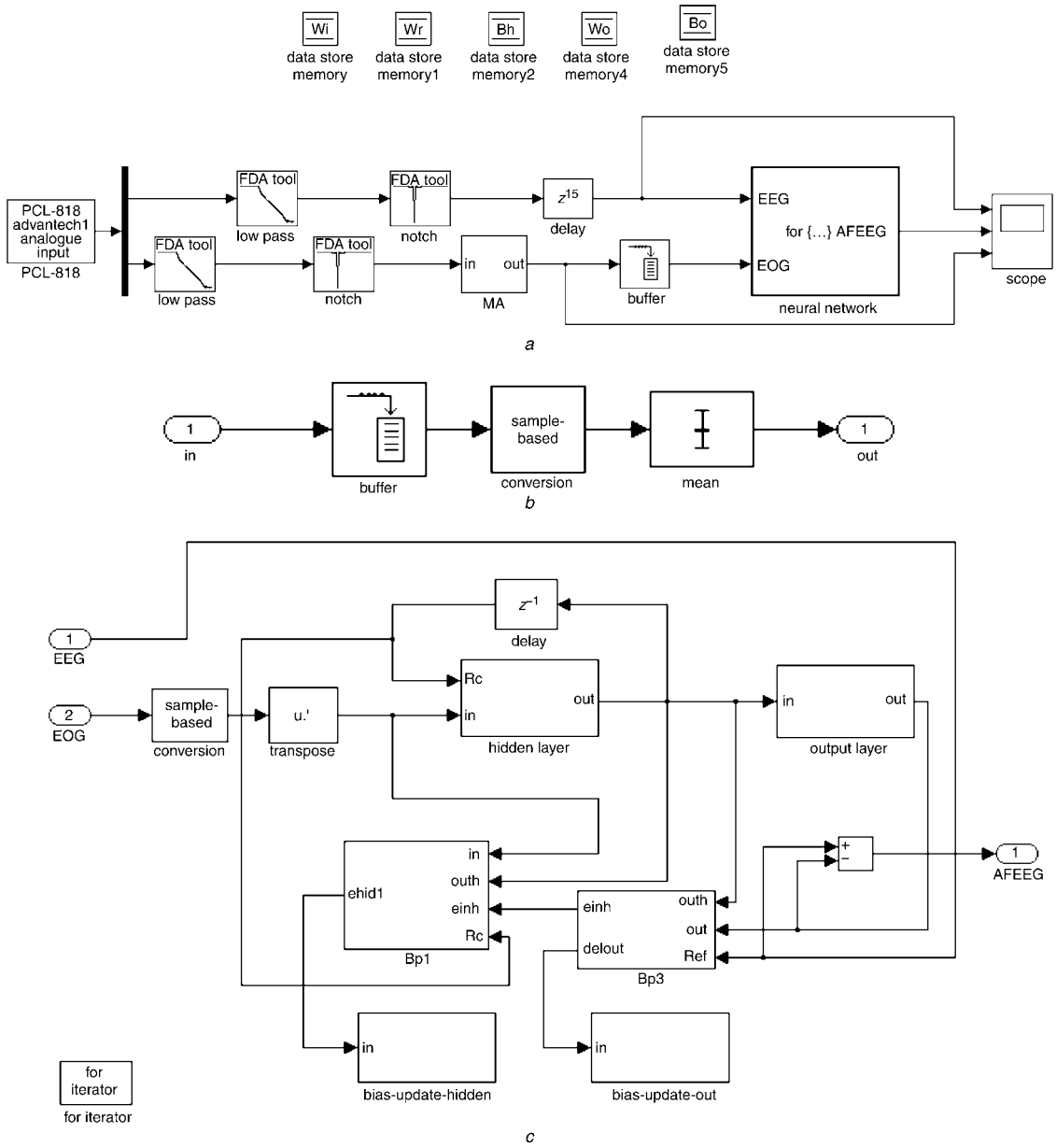

Fig. 10 *Matlab Simulink block diagram of (a) NANC, (b) recurrent neural network and (c) moving averaged filter*

eye blink and eye movement artifacts were recorded by placing an electrode on the forehead above the left brow line and an electrode on the left temple. All recording channels were referenced to the right earlobe. The signals were continuously collected and processed, while the subject was free to blink and to move his eyes. The measured values were low-pass filtered (cutoff frequency = 40 Hz). The NANC described above was used for *real-time ocular artifact suppression.* The primary signal was the measured EEG data from position F3. The reference signal was the data recorded from the forehead electrode when the eye did not move, and the eye blink artifacts were going to be suppressed. During the removal of eye blink and eye movement artifacts, the reference signal was generated by the adding of the data recorded from the forehead electrode to the data recorded from the temple electrode. The output of the neural network was an estimate of the noise in the primary signal, and the output of the NANC was an estimate of the artifact-free EEG. The NANC was here implemented by means of a recurrent neural network with four input nodes, eight hidden units and one output node. The learning rate was chosen as 0.01. It should be noted that the leaning process never stops and continuously adapts the free parameters of the network to variations in the incoming signals.

Fig. 10*a* shows the Matlab Simulink block diagram of the NANC for real-time *ocular artifact suppression.* The neural network and the moving window average filter were implemented by the Simulink blocks (Figs 10*b* and *c*). These blocks belong to the fundamental Matlab digital signal processor library and are coded in real-time workshop format to support real-time operation.

4.3 *Results*

Fig. 11*a* shows eye blink artifact suppression for a 10 s portion of the recorded EEG signals at frontal site F3 during the real-time mode of operation. It was observed that the eye blink artifacts were significantly suppressed by the NANC. Fig. 11*b* shows the same information as in Fig. 11*a* for a different portion of the recorded EEG. Although the structure of the eye blink artifacts is totally different, owing to a time-varying property, the proposed NANC can be used to remove

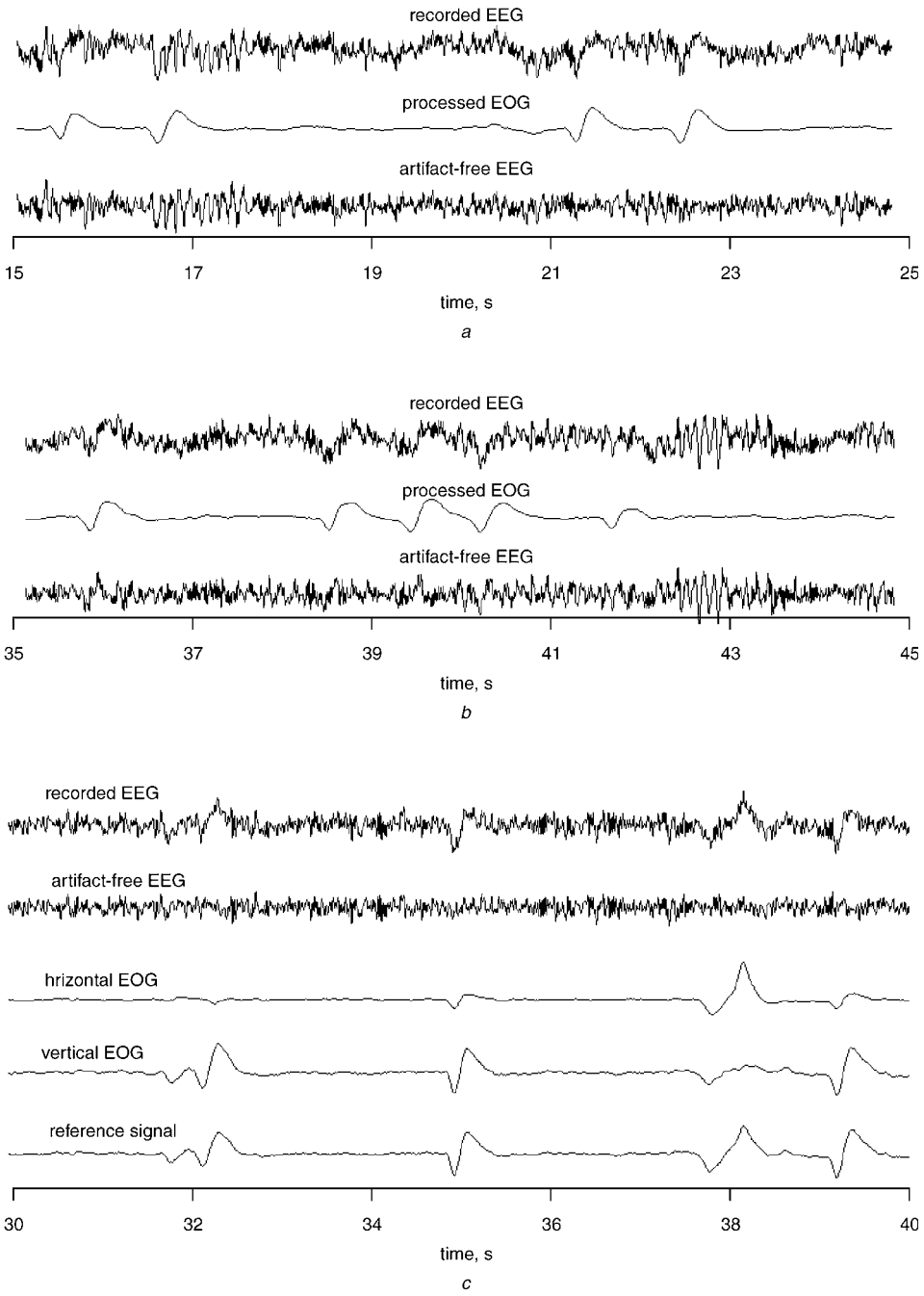

Fig. 11 *(a) Real-time eye blink artifact suppression for 10 s portion of recorded EEG signals at frontal site F3. Reference signal is data recorded from forehead electrode. (b) Same information as in (a) for different portion of recorded EEG. (c) Real-time eye movement and eye blink artifact suppression for 10 s portion of recorded EEG signals, while reference signal is generated by adding data recorded from forehead electrode to data recorded from temple electrode*

ocular artifacts from even strongly contaminated EEG recordings. Removal of eye movement artifacts is shown in Fig. 11*c*. In this case, the reference signal was generated by adding the data collected from the forehead electrode to the data recorded from the temple electrode. It was clearly observed that the eye movement artifacts were perfectly removed, as well as the eye blink artifacts.

Fig. 12 shows eye blink artifact suppression for different EEG channels during off-line operation using the NANC. The NANC was also here implemented by means of a recurrent neural network with four input nodes, eight hidden units and one output node. The learning rate was chosen as 0.005. During off-line operation, the network was considered to have converged when the absolute rate of change in the mean-squared error per epoch was sufficiently small. During each epoch, the whole recorded signal was applied to the NANC. It was observed that the ocular artifacts were perfectly removed, even with short-time recordings in EEG experimental sessions. Moreover, the baseline wander caused by the eye movements has been removed. It is important to note that the NANC does not distort the EEG when there is no artifact.

5 Conclusions

In this paper, we have presented a non-linear adaptive noise canceller using a recurrent neural network for real-time removal of the EOG interference from EEG signals. The results show that the ocular artifacts are perfectly removed even with a single-reference signal. The reference signal is generated by adding the data collected from the forehead electrode to the data recorded from the temple electrode. This is unlike the conventional eye blink and eye movement artifact recording, which

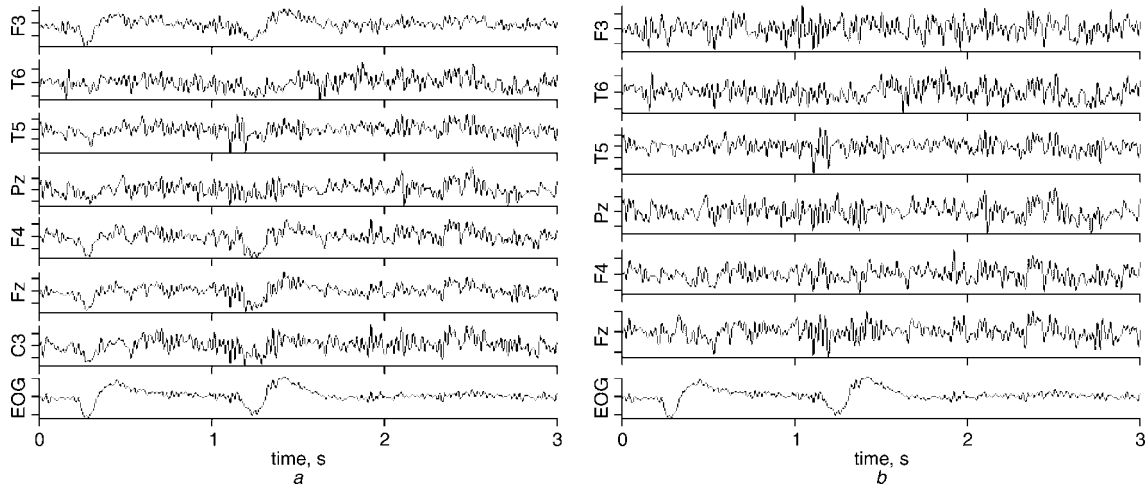

Fig. 12 *Eye blink suppression for different EEG channels during off-line operation: (a) recorded EEG signals; (b) artifact-free EEG signals*

uses two pairs of electrodes: one pair of electrodes are placed above and below the eye to record the vertical EOG, and another pair are placed at the left and right outer canthi to record horizontal EOG.

In addition to the ability of real-time suppression, the proposed scheme would be able to remove ocular artifacts from contaminated EEG signals during short experimental sessions. This is another factor of concern during the training phase of BCI. Moreover, it is found that eye blink variability does not affect the performance of the NANC.

In this paper, we used a recurrent neural network for modelling the noise component in the primary signal and compared its performance with that of a feedforward neural network. Recurrent neural networks (RNNs) are biologically more plausible and computationally more powerful than feedforward networks, and their use is very appropriate for modelling nonlinear dynamic systems. The RNN used in this paper consists of an input source node, a single hidden layer and one linear output node. This simple structure makes RLSP suitable for real-time applications.

References

ARABI, A., and ERFANIAN, A. (1999): 'Neural adaptive filters for estimating brainstem auditory evoked potential', *Proc. Int. Conf. IEEE/EMBS*, Atlanta, GA, USA, **20**, p. 431

BERG, P., and SCHERG, M. (1991): 'Dipole models of eye activity and its application to the removal of eye artifacts from the EEG and MEG', *Clin. Physiol. Meas.*, **12**, pp. 49–54

BERG, P., and SCHERG, M., (1994): 'A multiple source approach to the correction of eye artifacts', *Electroenceph. Clin. Neurophysiol.*, **90**, pp. 229–241

CHAN, F. H. Y., LAM, F. K., POON, P. W. F., and QIU, W. (1995): 'Detection of brainstem auditory evoked potential by adaptive filtering', *Med. Biol. Eng. Comput.*, **33**, pp. 69–75

CONNOR, J. T., MARTIN, R. D., and ATLAS, L. E. (1994): 'Recurrent neural networks and robust time series prediction', *IEEE Trans. Neural Netw.*, **5**, pp. 240–254

DENG, Y., WOLF, W., SCHNELL, R., and APPEL, U. (2000): 'New aspects to event-synchronous cancellation of ECG interface: an application of the method in diaphragmatic EMG signals', *IEEE Trans. Biomed. Eng.*, **47**, pp. 1177–1184

ERFANIAN, A., and MAHMOUDI, B. (2002): 'Real-time eye blink suppression using neural adaptive filters for EEG-based brain computer interface', *Proc. Int. Conf. IEEE/EMBS*, Houston, USA, **1**, pp. 44–45

GILES, C. L., KUHN, G. M., and WILLIAMS, R. J. (1994): 'Dynamic recurrent neural networks: theory and applications', *IEEE Trans. Neural Netw.*, **5**, pp. 153–156

GRATTON, G., COLES, M. G., and DONCHIN, E. (1983): 'A new method for off-line removal of oucular artifact', *Electroencephalogr. Clin. Neurophysiol.*, **55**, pp.486–484

GRIEVE, R., PARKER, P. A., HUDGINS, B., and ENGLEHART, K. (2000): 'Nonlinear adaptive filtering of stimulus artifact', *IEEE Trans. Biomed. Eng.*, **47**, pp. 389–395

HAYKIN, S. (1999): 'Neural networks: A comprehensive foundation' (Prentice-Hall, 1999)

HE, P., WILSON, G., and RUSSELL, C. (2004): 'Removal of ocular artifacts from electro-encephalogram by adaptive filtering', *Med. Biol. Eng. Comput.*, **42**, pp. 407–412

JAMES, C. J., HAGAN, M. T., JONES, R. D., BONES, P. J., and CARROLL, G. J. (1997): 'Multireference adaptive noise cancelling applied to the EEG', *IEEE Trans. Biomed. Eng.*, **44**, pp. 775–779

JUNG, T., MAKEIG, S., HUMPHRIES, C., LEE, T., MCKEOWN, M. J., IRAGUI, V., and SEJNOWSKI, T. J. (2000): 'Removing electroencephalographic artifacts by blind source separation', *Psychophysiology*, **37**, pp. 163–178

LAGUNA, P., JANE, R., MESTE, O., POON, P. W., CAMINAL, P., RIX, H., and THAKOR, N. V. (1992): 'Adaptive filter for event-related bioelectric signals using an impulse correlated reference input: comparison with signal averaging techniques', *IEEE Trans. Biomed. Eng.*, **39**, pp. 1031–1044

LINS, O. G., PICTON, T. W., BERG, P., and SCHERG, M., (1993): 'Ocular artifacts in recording EEG and event-related potentials potentials II: Source dipoles and source components", *Brain Topogr.*, **6**, pp. 65–78

MAKEIG, S., BELL, A. J., JUNG, T. P., and SEJNOWSKI, T. J. (1996): 'Independent component analysis of electroencephalographic data', *Adv. Neural Info. Process. Syst.*, **8**, pp. 145–151

MATHEWS, V. J. (1991): 'Adaptive polynomial filters', *IEEE Signal Process. Mag.*, **5**, pp. 10–26

PARSA, V., PARKER, P. A., and SCOTT, R. (1998): 'Adaptive stimulus artifact reduction in noncortical somatosensory evoked potential studies', *IEEE Trans. Biomed. Eng.*, **45**, pp. 165–179

QUI, W., FUNG, K. S. M., CHAN, F. H. Y., LAM, F. K., POON, P. W. F., and HAMERNIK, R. P. (2002): 'Adaptive filtering of evoked potentials with radial-basis-function neural network prefilter', *IEEE Trans. Biomed. Eng.*, **49**, pp. 225–232

RAUF, F., and AHMED, H. M. (1997): 'New nonlinear adaptive filters with applications to chaos', *Int. J. Bifurcation Chaos*, **7**, pp. 1791–1809

SADASIVAN, P. K., and DUTT, D. N. (1997): 'Development of Newton--type adaptive algorithm for minimization of EOG artifacts from noisy EEG signals', *Signal Process.*, **62**, pp. 173–186

STROBACH, P., ABRAHAM-FUCHS, K., and HARER, W., (1994): 'Event-synchronous cancellation of the heart interference in biomedical signals', *IEEE Trans. Biomed. Eng.*, **41**, pp. 343–350

THAKOR, N. V., and Yi-Sheng, Z. (1991): 'Applications of adaptive filtering to ECG analysis: noise cancellation and arrhythmia detection', *IEEE Trans. Biomed. Eng.*, **38**, pp. 785–794

THE MATHWORKS, INC., (1990–2001): 'Using Simulink', (THE MATHWORKS, INC., 1994–2001)

THE MATHWORKS, INC., (1999–2000): 'Real-Time Windows Target User's Guide', (THE MATHWORKS, INC., 1999–2000)
TSOI, A. C., and BACK, A. D. (1994): 'Locally recurrent globally feedforward networks: a critical review of architectures', *IEEE Trans. Neural Netw.*, **5**, pp. 229–239
VIGARIO, R. N. (1997): 'Extraction of ocular artifacts from EEG using independent component analysis', *Electroenceph. Clin. Neurophysiol.*, **103**, pp. 395–404
WIDROW, B., and STREANS, S. D., (1985): 'Adaptive signal processing', (Prentice-Hall, Englewood Cliffs, NJ, 1985)
WOESTENBURG, J. C., VERBATEN, M. N., and SLANGEN, J. L., (1983): 'The remaoval of the eye-movement artifact from the EEG by regression analysis in the frequency domain', *Biol. Psych.*, **16**, pp. 127–147
YU, X., HE, Z., and ZHANG, Y. (1994): 'Time-varying adaptive filters for evoked potential estimation', *IEEE Trans. Biomed. Eng.*, **41**, pp. 1062–1071

Author's biography

ABBAS ERFANIAN received the B.S. degree in computer engineering from Shiraz University, Shiraz, in 1985, the M.S. degree in computer engineering from Sharif University of Technology, Tehran, in 1989, the PhD degree in biomedical engineering from Tarbiat Modarres University, Tehran, Iran in 1995. In 1993 he was a Senior Research Associate at Case Western Reserve University and VA Medical Center, Cleveland, OH, where he did research in the area of functional electrical stimulation, and neuromuscular control systems. Since 1995, he has been Assistant Professor of Biomedical Engineering at Iran University of Science and Technology. He currently teaches graduate courses on biomedical signal processing, biological system modeling, neural network, and neuro-muscular control systems.